Why Do C_1-Symmetric *ansa*-Zirconocene Catalysts Produce Lower Molecular Weight Polymers for Ethylene/Propylene Copolymerization than for Ethylene/Propylene Homopolymerization?

Dongqi Wang,[†] Simone Tomasi,[†] Abbas Razavi,[‡] and Tom Ziegler*[,†]

Department of Chemistry, University of Calgary, 2500 University Drive NW, Calgary, Alberta, Canada T2N 1N4, and Total Petrochemicals Research Feluy, Zone Industrielle C, B-7181 Seneffe (Feluy), Belgium

Received April 1, 2008

We have carried out a combined QM/MM study to rationalize the factors that can affect the performance of C_1-symmetric *ansa*-zirconocene catalysts that contain bridged cyclopentadienyl (Cp) and fluorenyl (Flu) ligands in olefin homo- and copolymerization. Two growing chains with different β-C (tertiary or secondary) and two olefins (propene and ethylene) have been used for this purpose. Our calculations indicate that chain transfer has a higher barrier than chain propagation in EE (ethylene homopolymerization), PP (propylene homopolymerization), and PE (propylene complexation to a metal with a propyl chain) systems. However, the two processes are competitive in EP (ethylene complexation to a metal with a 2-methylpropyl chain) system. Substituents on the carbon in a C−H link weaken the C−H bond. This in turn determines the order EP < EE < PP < PE for the heat of reaction of the β-hydrogen transfer process, giving rise to the chain termination, where the process with the most negative reaction heat is the more thermodynamically favorable. It is further argued that the barriers for the termination process must follow the same order of EP < EE < PP < PE. For the insertion process the barrier increases with the number of substituents on the olefin and the C^{β} atom of the growing chain as PP > PE ∼ EP > EE. The different propensity of the four systems for termination and propagation results in the higher barrier of termination for EE, PP, and PE, whereas the barriers are similar for EP. Our analysis explains why ethylene/propylene homopolymerization affords high molecular weight polymers, whereas ethylene/propylene copolymerization affords low molecular weight polymers.

Introduction

The past two decades have seen a remarkable growth and development in the field of olefin polymerization based on single-site homogeneous catalysts that are able to produce polymers with high stereoselectivity and a narrow molecular weight distribution.[1–3] Single-site catalysts are also easy to characterize, which makes it possible to study the polymerization process in considerable mechanistic detail.[3–5]

Metallocene-containing catalysts are one important family of single-site homogeneous catalysts. The typical feature of these compounds is the sandwich topology in which a transition metal (Zr, Hf, etc.) is coordinated to two (substituted) cyclopentadienyl groups (Cp, fluorenyl, etc.). The two ligands can be connected by one or two C/Si bridges, which increase the internal torsion strength compared to the unbridged systems.

Following the report on C_s-symmetric fluorenyl-containing metallocenes of the type (η^5-$C_5H_4CMe_2$-η^5-$C_{13}H_8$)MCl_2 (M = Zr, Hf),[6,7] C_1-symmetric catalysts have been developed with different substituents on the cyclopentadienyl (Cp) and/or fluorenyl (Flu) groups.[3,8,9] In these *ansa* complexes, the η^5-cyclopentadienyl and η^5-fluorenyl rings are bridged by an isopropylidene group. The development of these catalysts has made it possible to synthesize syndiotactic polymers from propylene. On the other hand, C_2-metallocenes are found to be efficient catalysts in the production of isotactic polypropylene polymers with high molecular weights and melting point.[9]

While the C_1-symmetric zirconocene (η^5-3-*t*-Bu-5-Me-C_5H_2-$C(Me_2)$-η^5-3,6-di-*t*-Bu-$C_{13}H_6$)MCl_2 precatalysts give rise to high molecular weight polymers in homopolymerization, they afford only low molecular weight polymers in copolymerization. This is a serious drawback that limits the use of single-site catalysts in olefin polymerization. Molecular weight is controlled by the relative rate of chain propagation and chain termination, where the latter process is represented by β-hydrogen transfer to monomer.[10] It is the objective of the current study to examine

* Corresponding author. E-mail: ziegler@ucalgary.ca.
[†] University of Calgary.
[‡] Total Petrochemicals Research Feluy.

(1) Alt, H. G.; Köppl, A. *Chem. Rev.* **2000**, *100*, 1205.
(2) Resconi, L.; Cavallo, L.; Fait, A.; Piemontesi, F. *Chem. Rev.* **2000**, *100*, 1253.
(3) Razavi, A.; Thewalt, U. *Coord. Chem. Rev.* **2006**, *250*, 155, and references therein.
(4) Tomasi, S.; Razavi, A.; Ziegler, T. *Organometallics* **2007**, *26*, 2024.
(5) Graf, M.; Angermund, K.; Fink, G.; Thiel, W.; Jensen, V. R. *J. Organomet. Chem.* **2006**, *691*, 4367.
(6) Ewen, J. A.; Jones, R. L.; Razavi, A.; Ferrara, J. D. *J. Am. Chem. Soc.* **1988**, *110*, 6255.
(7) Razavi, A.; Ferrara, J. *J. Organomet. Chem.* **1992**, *435*, 299.
(8) Miller, S. A.; Bercaw, J. E. *Organometallics* **2006**, *25*, 3576.
(9) Razavi, A.; Bellia, V.; Baekelmans, D.; Slawinsky, M.; Sirol, S.; Peters, L.; Thewalt, U. *Kinet. Catal.* **2006**, *47*, 257.
(10) Friederichs, N.; Wang, B.; Budzelaar, P. H. M.; Coussens, B. B. *J. Mol. Catal. A: Chem.* **2005**, *242*, 91.
(11) Kravchenki, R.; Waymouth, R. M. *Macromolecules* **1993**, *31*, 1.
(12) Tang, L.-M.; Li, Y.-G.; Ye, W.-P.; Li, Y.-S. *J. Polym. Sci. A1* **2006**, *44*, 5846.

10.1021/om800290n CCC: $40.75
Publication on Web 05/20/2008

Scheme 1. Schematic Representation of the Chain Propagation and β-H Transfer Reactions (the counteranion and bridged ligands are not shown for clarity)

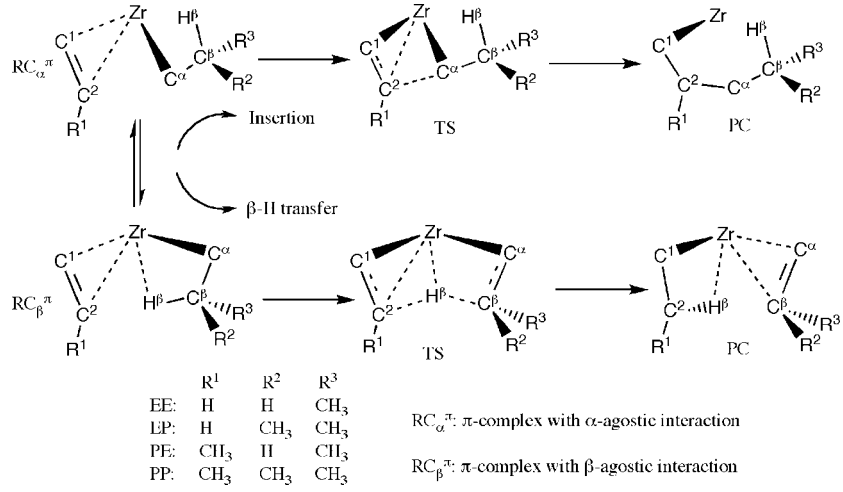

why the rate of chain termination in copolymerization becomes comparable to chain propagation with low molecular weight polymers as a result.

For this purpose, we have conducted a QM/MM investigation to unravel the factors that control the chain termination reaction in ethylene/propylene copolymerization catalyzed by C_1-symmetric zirconocenes. Four model processes have been investigated: homopolymerization of ethylene (EE), homopolymerization of propene (PP), copolymerization of ethylene and propene with ethylene insertion after propene insertion (EP), and compolymerization of ethylene and propene with propene insertion after ethylene insertion (PE) (see Scheme 1).

Computational Details

We have carried out DFT/MM calculations to rationalize the factors that affect the performance of C_1-symmetric zirconocene-containing catalyst [Me_2C(3-*t*-Bu-5-Me-C_5H_2)(3,6-di-*t*-Bu-$C_{13}H_6$)-$ZrCH_3$]$^+$[$CH_3B(C_6F_5)_3$]$^-$ in homo- and copolymerization. The three *tert*-butyl groups on the bridged ligand together with the three C_6F_5 groups of the anion were defined as the MM region, and the other part of the model system, including the growing chain, the olefin, and the zirconocene complex without the three *tert*-butyl groups and BCH_3 moiety of the anion, was put in the QM region. The C_6F_5 groups were in the QM region represented by Cl capping atoms, which is well validated in previous work,[22] whereas hydrogens were used as capping atoms for the *tert*-butyl groups.

The ADF program[23] was used for the calculations, and a well-tested density functional theory (BP86)[24] method was employed for the treatment of the QM region, with a Sybyl/TRIPOS 5.2 force field[25] describing the MM region. The energies were calculated by adopting the IMOMM scheme[26] as implemented in ADF.[27]

Double-ζ STO basis sets with a single polarization function were employed for the H, B, C, F, and Cl atoms, while a triple-ζ STO basis set with one p-type polarization function was employed for Zr. The 1s electrons of B and C, the 1s−2p electrons of Cl, and the 1s−3d electrons of Zr were treated as frozen core. First-order scalar relativistic corrections were applied to the systems studied.[28–30]

All optimizations of the stationary points reported here were done in gas phase without any constraint. We have in the present work explored and compared the energies of the insertion (propagation) and β-H transfer (chain termination) reactions. All energies are given in kcal/mol and are from the calculations with anion included unless stated otherwise.

Results and Discussion

A. Zirconocene and Zirconocene−Olefin π-Complexes. The actual metallocene catalyst is generated by activating an alkylated form of the precursor compound, with a Lewis acid or cocatalyst, e.g., tri(pentafluoro)phenylborate ($B(C_6F_5)_3$) in our model system. The activation starts from the methylation of a dichloride derivative, followed by methide abstraction by the Lewis acid to give the metallocene monomethyl cation and the methylated anion.[1] The cation is the species that is responsible for the catalytic activity. As proposed previously,[13–21] the counteranion does not leave the zirconocene cation, but forms together with it an ion pair. To take into account the effect of the counteranion A^-, we have included one molecule of tri(pentafluoro)phenylmethylborate [$CH_3B(C_6F_5)_3$]$^-$ to model the counteranion A^- in the reaction system. Thus in our calculations the whole catalytic system is denoted as [Cat^+][A^-], which is taken as the resting state for the catalytic system (Figure 1).

(13) Chen, E. Y.-X.; Marks, T. J. *Chem. Rev.* **2000**, *100*, 1391.
(14) Lanza, G.; Fragala, I. L.; Marks, T. J. *J. Am. Chem. Soc.* **1998**, *120*, 8257.
(15) Fusco, R.; Longo, L.; Proto, A.; Masi, F.; Garbassi, F. *Macromol. Rapid Commun.* **1998**, *19*, 257.
(16) Nifant'ev, I. E.; Ustyyuk, L. Y.; Laikov, D. N. *Organometallics* **2001**, *20*, 5375.
(17) Xu, Z.; Vanka, K.; Ziegler, T. *Organometallics* **2004**, *23*, 104.
(18) (a) Bernardi, E.; Bottoni, Z.; Miscione, G. P. *Organometallics* **1998**, *17*, 16. (b) Schaper, F.; Geyer, A.; Brintzinger, H. H. *Organometallics* **2002**, *21*, 473.
(19) Yang, X.; Stern, C. L.; Marks, T. J. *J. Am. Chem. Soc.* **1994**, *116*, 10015.
(20) Deck, P. A.; Marks, T. J. *J. Am. Chem. Soc.* **1995**, *117*, 6128.
(21) Vanka, K.; Chan, M. S. W.; Pye, C. C.; Ziegler, T. *Organometallics* **2000**, *19*, 1841.
(22) Vanka, K.; Xu, Z.; Ziegler, T. *Can. J. Chem.* **2003**, *81*, 1413.
(23) (a) te Velde, G.; Bickelhaupt, F. M.; van Gisbergen, S. J. A.; Fonseca Guerra, C.; Baerends, E. J.; Snijders, J. G.; Ziegler, T. *J. Comput. Chem.* **2001**, *22*, 931. (b) Fonseca Guerra, C.; Snijders, J. G.; te Velde, G.; Baerends, E. J. *Theor. Chem. Acc.* **1998**, *99*, 391.
(24) (a) Becke, A. D. *Phys. Rev. A* **1988**, *38*, 3098. (b) Perdew, J. P. *Phys. Rev. B* **1986**, *33*, 8822. (c) Erratum: Perdew, J. P. *Phys. Rev. B* **1986**, *34*, 7406.
(25) Clark, M.; Cramer, R. D. I.; van Opdenbosch, N. *J. Comput. Chem.* **1989**, *10*, 982.
(26) Morokuma, K.; Maseras, F. *J. Comput. Chem.* **1995**, *117*, 5179.
(27) Woo, T. K.; Cavallo, L.; Ziegler, T. *Theor. Chem. Acc.* **1998**, *100*, 307.
(28) Snijders, J. G.; Baerends, E. J.; Ros, P. *Mol. Phys.* **1979**, *38*, 1909.

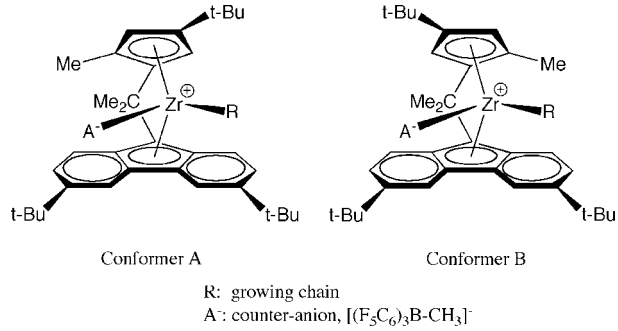

Figure 1. Resting state for the ion pair: conformers A and B.

Table 1. Key Geometrical Parameters[a] for Conformers[b] A and B

conformer	$Zr-C_\alpha^{anion}$	$Zr-C_\alpha^{chain}$	$C_\alpha^{anion}-B$	energy
A	2.527	2.262	1.651	0.00
B	2.530	2.252	1.649	−2.06

[a] Bond lengths in Å, energy in kcal/mol. $Zr-C_\alpha^{anion}$ is the distance between Zr and the bridging C atom of the anion, $Zr-C_\alpha^{chain}$ is the distance between Zr and the α-C of the growing chain, and $C_\alpha^{anion}-B$ is the distance between the bridging C atom and the boron atom of the anion. [b] For conformers A and B see Figure 1.

In the ion pair, the counteranion occupies one coordination position of Zr, with a Zr−C distance of 2.5−2.6 Å. The anion generates steric hindrance, which blocks the entry of monomers into the active site.

We display in Figure 1 two conformers for the catalytic ion pair that differ through the binding mode of the counteranion, in which the growing chain is modeled by an iso-butyl group. In conformer A, the counteranion is trans to the *tert*-butyl group on the cyclopentadienyl ligand (Cp). In this conformer, the growing chain extends between the two *tert*-butyl groups, suffering considerable repulsive interaction.[9] In conformer B, the counteranion is cis to the *tert*-butyl group of the cyclopentadienyl ligand. In this conformer, the growing chain does not feel as strongly the repulsive interaction from the Cp ligand.

Selected parameters of the two optimized conformers are tabulated in Table 1 for comparison. We can see that the bonding between Zr and the growing chain is somewhat stronger in conformer B (bond length shorter by 0.01 Å), while the interaction between Zr and the counteranion is similar in both conformers in view of the distance between Zr and the CH_3^- bridge of the counteranion. Energetically, conformer B is more stable than A by 2 kcal/mol. Therefore, our calculations suggest that conformer B is the more favorable conformation for the resting state. In the following calculations we have adopted conformer B as the starting species involved with the uptake of the monomer and the insertion/β-H transfer reactions.

In the resting state (B of Figure 1), the active site is crowded with four ligands: two substituted cyclopentadienyl groups, the growing chain, and the counteranion, leaving no space for olefin to bind. Thus, it is conceivable that the uptake of olefin will compete with the formation of the ion pair, and the binding of olefin to Zr will weaken the interaction between Cat^+ and A^-, leading to the displacement of the counteranion. In principle, the entry of the monomer can follow two routes: *cis* and *trans* to the counteranion. The *trans* path requires the adjustment of the growing chain in addition to the displacement of the counteranion and thus is more energy-demanding compared to the *cis* approach path. On the basis of this knowledge and previous studies as well,[31] we have concentrated on the *cis* approach of the olefin.

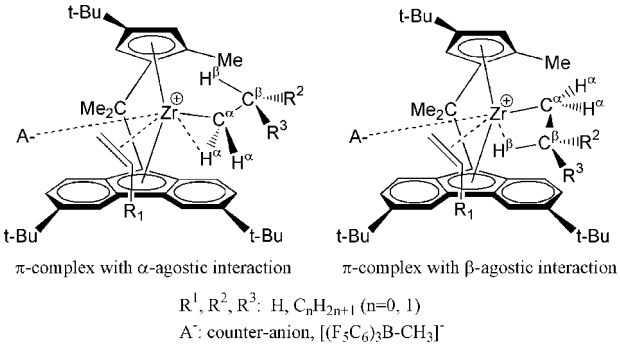

Figure 2. π-Complexes: RC_α^π vs RC_β^π.

Table 2. Relative Energies for the Four Model Systems with the Anion Included

	RC_α^π	RC_β^π	TS-bH	PC-bH	TS-Ins	PC-Ins
EE_cis	0.00	0.38	7.38	−2.18	2.69	−8.35
PP_cis	0.00	0.78	10.85	−0.97	6.70	−2.74
EP_cis	0.00	−1.61	4.25	−7.16	4.36	−9.64
PE_cis	0.00	1.57	13.10	3.81	5.53	−4.33

A schematic representation of the π-complexes with olefin bound to Zr is shown in Figure 2. In the π-complex, Zr is coordinated to four different groups (olefin, cyclopentadiene, growing chain, and Flu); thus Zr is a chiral center. Following the Cahn−Ingold−Prelog conventions (CIP), the complexes have R chirality around the metal center. The two π-complexes shown in Figure 2 differ in the formation of an agostic interaction between Zr and β-H of the growing chain. In the case where there is no β-agostic interaction possible, we observe instead a weak agostic interaction between Zr and an α-H of the growing chain.

B. Chain Propagation vs Chain Transfer. We shall now turn to a study of chain propagation and chain transfer. In principle, there are two possible routes that olefin insertion may follow: 1,2-insertion (regioregular) and 2,1-insertion (regioerror). For early transition metal systems studied here, 1,2-insertion is favored according to both experimental[9] and theoretical[2] studies. We shall thus consider only propagation and termination following 1,2-insertion.

The transition state for the chain propagation was located with the help of the reaction coordinate $d_{C^\alpha-C^2}$ (C^α: α-C of growing chain, C^2: β-C of monomer) starting from the π-complex, while the transition state for the β-H transfer reaction was located with the help of the reaction coordinate $d_{C^\beta-H} - d_{H-C^2}$ (C^β: β-C of growing chain, C^2: β-C of monomer); thus the cleavage of the $C^\beta_{chain}-H^\beta$ bond and the formation of the $C^\beta_{olefin}-H^\beta$ bond were considered a concerted process. The relative energies obtained from full optimizations are collected in Table 2, and we display in Figure 3 the geometrical parameters for the insertion and termination processes including the PP and EP systems.

EE_System: Ethylene Homopolymerization. We shall start with the insertion of ethylene into a primary alkyl chain. Figure 4 displays the potential energy profile for ethylene insertion starting at the π-complex with an α-agostic interaction, RC_α^π.

According to our calculations (see Table 2 and Figure 4), the barrier for the propagation step is 2.70 kcal/mol (TS-Ins),

(29) Boerrigter, P. M.; Baerends, E. J.; Snijders, J. G. *Chem. Phys.* **1988**, *122*, 357.
(30) Ziegler, T.; Tschinke, V.; Baerends, E. J.; Snijders, J. G.; Ravenek, W. *J. Phys. Chem.* **1989**, *93*, 3050.
(31) Yang, S.-Y.; Ziegler, T. *Organometallics* **2006**, *25*, 887.
(32) Michalak, A.; Ziegler, T. *Organometallics* **1999**, *18*, 3998.

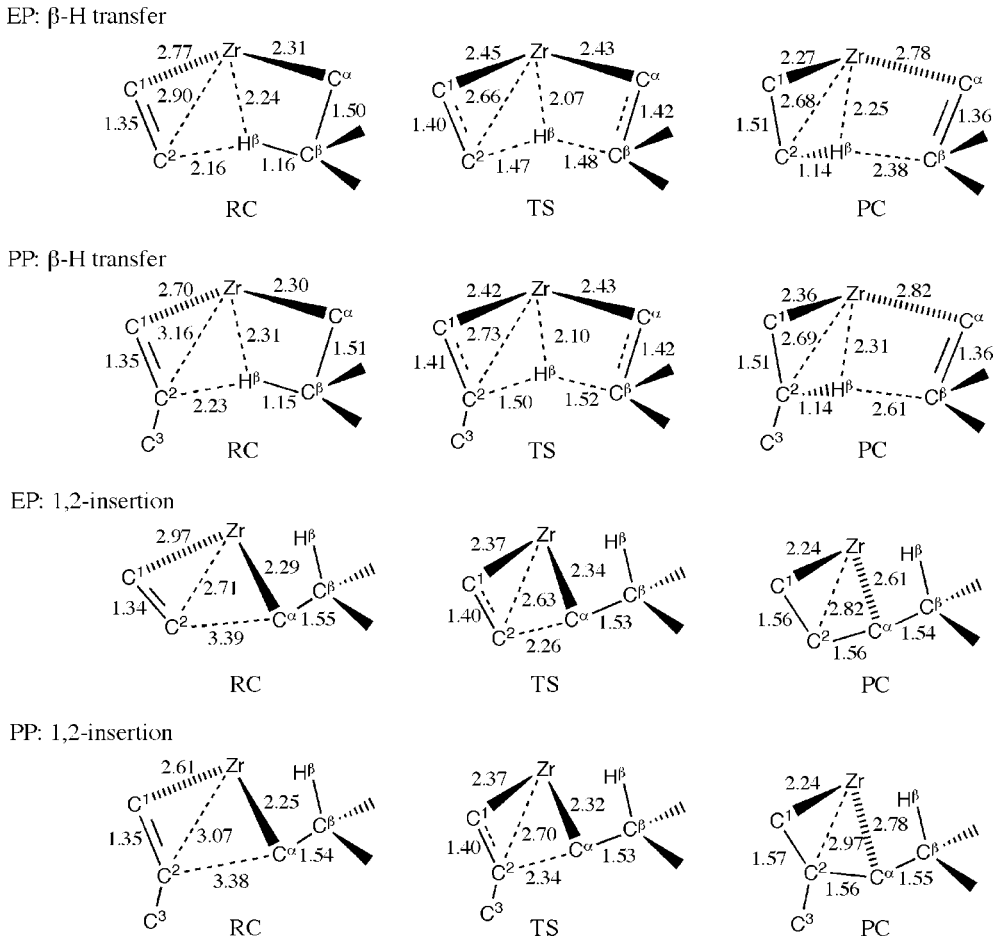

Figure 3. Insertion vs β-H transfer for EP and PP systems: geometrical parameters.

while the barrier for the β-H transfer is as high as 7.38 kcal/mol (TS-bH). In addition, the two processes are found to be exothermic by 8.35 and 2.18 kcal/mol for chain propagation (PC-Ins) and chain transfer (PC-bH) respectively. Thus, the chain transfer is not as favorable as the insertion either kinetically or thermodynamically.

In the calculations on the β-H transfer, before approaching the transition state (TS-bH), there is a change in conformation from the π-complex RC_α^π with a $Zr-H^\alpha$ bond to a π-complex with an agostic interaction between Zr and $C^\beta-H^\beta$ of the growing chain (RC_β^π). The newly formed RC_β^π is found to be some 0.38 kcal/mol less stable. Over the remaining part of the β-H transfer, the β-agostic interaction is conserved, with the distance $Zr-H^\beta$ being within 2.2−2.4 Å, implying a metal assistance of the β-H transfer. The agostic interaction contributes to the cleavage of the $C^\beta_{chain}-H^\beta$ bond and the formation of the $C^2_{olefin}-H^\beta$ bond.

PP_System: Propene Homopolymerization. For propene insertion into the alkyl chain with a tertiary β-C we find a barrier for the propagation step of 6.70 kcal/mol, while the barrier for the β-H transfer is higher, at 10.85 kcal/mol. In addition, the two processes are found to be exothermic by 2.74 and 0.97 kcal/mol, respectively. Thus the chain transfer is not competitive with the insertion step on kinetic grounds. The potential energy surface is shown schematically in Figure 5.

Similar to the EE system, an intermediate (RC_β^π) with an agostic interaction between a β-H and Zr is observed prior to approaching the transition state (TS-bH) in the calculations on β-H transfer (see Figure 5). This intermediate is calculated to be 0.78 kcal/mol less stable than the π-complex with the α-agostic interaction (RC_α^π) (see Table 2).

EP_System: Ethylene as Comonomer after Propene Insertion. The EP system displays some features different from the EE and PP complexes. For the EP system the π-complex with a β-agostic interaction between Zr and the β-H of the growing chain is found to be more stable than the π-complex with an α-agostic interaction by 1.61 kcal/mol. Thus, the studies for the EP system start from the π-complex with an agostic interaction between Zr and the β-H of the growing chain.

The potential energy surfaces for insertion and β-H transfer are plotted in Figure 6. As seen from the figure, the barrier to the β-H transfer is calculated to be 5.86 kcal/mol, comparable to that for the insertion pathway of 5.97 kcal/mol (relative to RC_β^π). The reaction energies for both processes are also comparable with the values of −8.03 and −5.55 kcal/mol for insertion and β-H transfer, respectively. Thus, for the EP_system, the chain transfer is kinetically competitive with the insertion step.

PE_System: Propylene as Comonomer after Ethylene Insertion. In this model system, the growing chain has a secondary β-C, as in the EE_system, and propylene works as the comonomer. The potential energy surfaces for the two reactions are plotted in Figure 7. According to our calculations, the barrier for the propagation step is 5.53 kcal/mol, while the barrier for the β-H transfer is as high as 13.10 kcal/mol. In addition, the two processes are found to be exothermic by 4.33

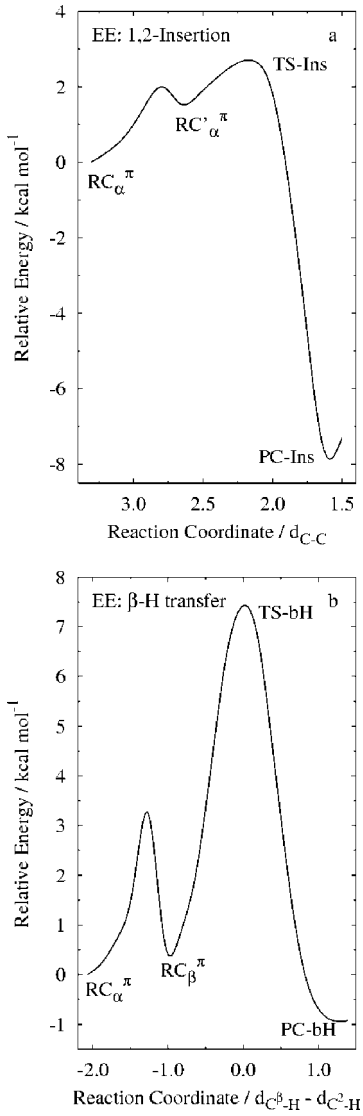

Figure 4. EE_system: olefin insertion (a) vs β-H transfer (b).

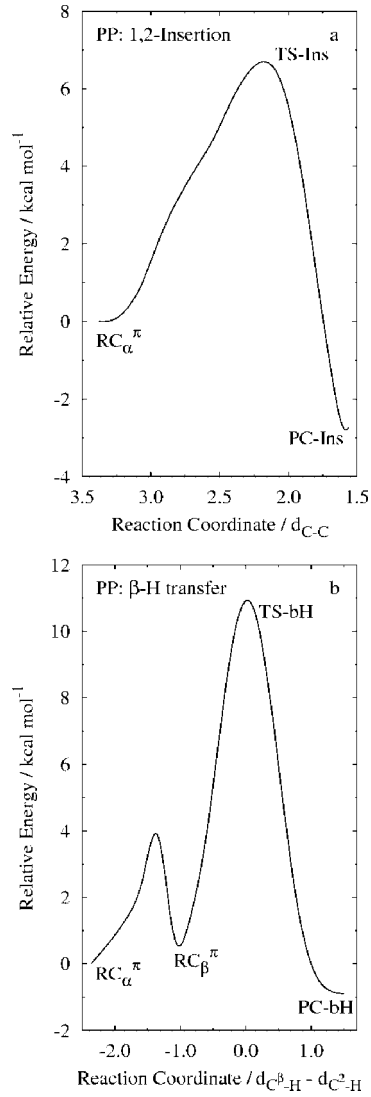

Figure 5. PP_system: olefin insertion (a) vs β-H transfer (b).

kcal/mol and endothermic by 3.81 kcal/mol. Clearly the chain transfer is kinetically strongly disfavored compared to chain propagation.

C. Analysis on Energies. The calculated energetics for the four model systems display different propensities for the β-H transfer pathway, as shown in Table 3, where we tabulated the reaction barriers and reaction enthalpies for this process.

As seen in Table 3, the reaction barrier increases from 4.25 to 13.10 kcal/mol in the order EP < EE < PP < PE; at the same time the heat of reaction increases from −7.16 to 3.81 kcal/mol. Considering first the EP system, the reaction involves the cleavage of a tertiary C−H bond and the formation of a primary C−H bond. Since the primary C−H bond is stronger than the tertiary C−H bond,[33] the reaction displays strong exothermicity (−7.16 kcal/mol). At the transition state (TS-bH), the partially formed primary C−H bond provides stabilization energy to compensate the energy required to break the tertiary C−H bond. The result is a lower barrier for the β-H transfer process in the case of EP than for the other systems to be discussed next.

In the EE system, a secondary C−H bond is broken and a primary C−H bond is formed. As the bond energy difference between secondary C−H and primary C−H bonds becomes smaller than between tertiary and primary C−H bonds, it leads to an increase in the reaction barrier and an increase of the reaction enthalpy compared to the EP system. The barrier is even higher for the PP system. Here a tertiary C−H bond is broken and a secondary bond formed with a marginally exothermic heat of reaction. In the PE system, since both the bond to be broken and the bond to be formed are secondary C−H bonds, the reaction has the highest reaction barrier of the four model systems under investigation, and it becomes an endothermic process.

The above analysis suggests that the reaction barrier and enthalpy strongly depend on the substituent groups that are attached to the carbon atoms between which the H^{β} atom migrates (C^2 of the olefin and C^{β} of the growing chain), as the substituents influence the C−H bond strengths.[33] We may use a schematic diagram to qualitatively describe this situation (Scheme 3).

In Scheme 3, the termination process is defined as a hydrogen transfer reaction between C^{β} (growing chain β-C) and C^2 (olefin carbon). Scheme 3a,b gives the estimate of the energy barrier for the H-transfer when C^2−H and C^{β}−H have similar bond strength (Scheme 3a) and different bond strength (Scheme 3b). We may thus expect lower barriers when the bond to be broken has a higher order C−H bond (with lower bond energy) than

(33) Mitoraj, M.; Zhu, H.; Michalak, A.; Ziegler, T. *J. Org. Chem.* **2006**, *71*, 9208.

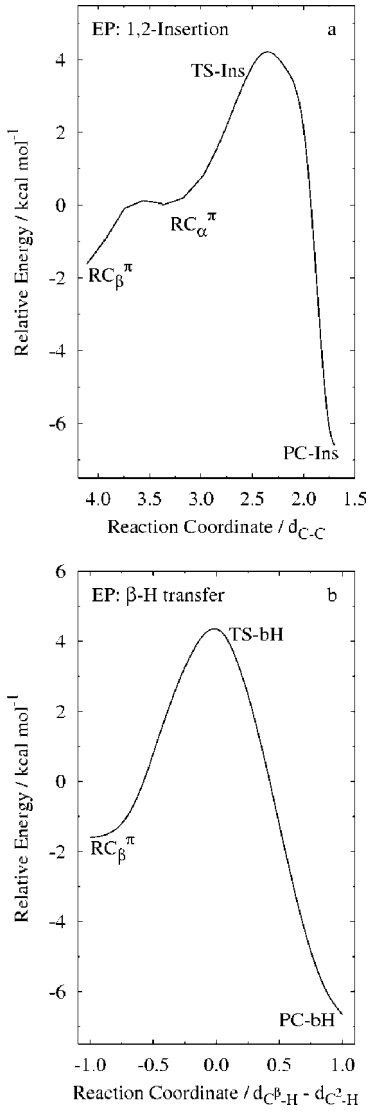

Figure 6. EP_system: olefin insertion (a) vs β-H transfer (b).

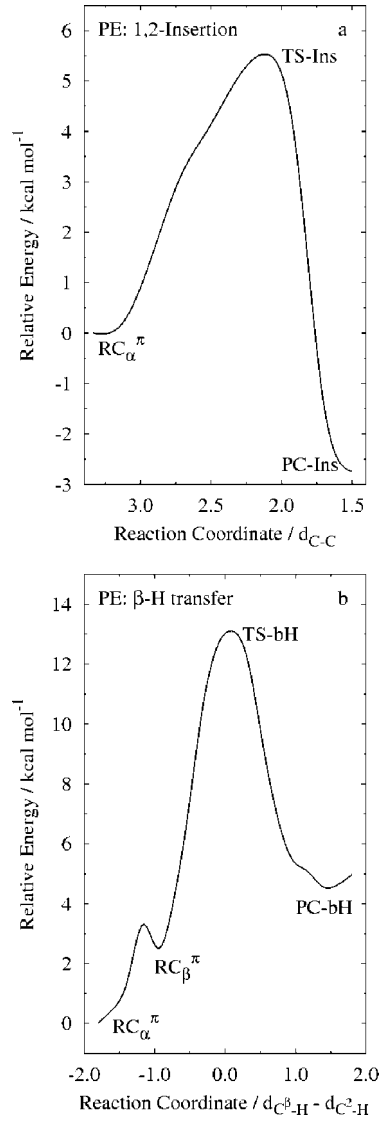

Figure 7. PE_system: olefin insertion (a) vs β-H transfer (b).

the bond to be formed (as in Scheme 3b). Also in this case the reaction is exothermic (as in the EP system). In contrast, if the cleaved bond has higher bond strength (as in the PE system), we have a higher barrier, as in the reverse reaction of Scheme 3b.

We have also carried out calculations without the anion, and we note the same dependence of $\Delta E^{\ddagger}$ and ΔH on the substituents R^1, R^2, R^3, and R^4 (Table 3). Thus, the trends in $\Delta E^{\ddagger}$ and ΔH should not be much influenced by the nature of A^-.

We note that in the 1,2-insertion reaction there is also a dependence of the energy barrier on the substituents of olefin and the growing chain. As it can be seen in Table 4, the EE system has the lowest energy barrier (2.69 kcal/mol), followed by EP (4.36 kcal/mol), PE (5.53 kcal/mol), and the PP (6.70 kcal/mol) systems. In these model systems, the number of methyl groups on olefin and the growing chain is 1, 2, 2, and 3, respectively. Therefore, our calculations suggest that the bulkier the substituents we find on C^2_{olefin} or C^{β}_{chain}, the higher the 1,2-insertion reaction barrier.

Table 3. Energetics vs Substituents on Olefin and Growing Chain in β-H Transfer[a]

	R^1	R^2	R^3	R^4	$\Delta E^{\ddagger b}$	ΔH^b	$\Delta E^{\ddagger c}$	ΔH^c
EP_cis	H	H	CH_3	CH_3	4.25	−7.16	2.46	−11.92
EE_cis	H	H	H	CH_3	7.38	−2.18	4.89	−6.40
PP_cis	H	CH_3	CH_3	CH_3	10.85	−0.97	8.68	−5.49
PE_cis	H	CH_3	H	CH_3	13.10	3.81	12.82	1.16

[a] For R^1, R^2, R^3, and R^4, see Scheme 2. [b] With counteranion. [c] Without counteranion.

Scheme 2. Active Region of the π-Complex in β-H Transfer

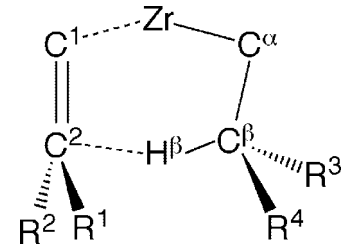

Concluding Remarks

We here reported a combined quantum mechanics and molecular mechanics (QM/MM) study on the chain propagation and termination processes in olefin homo- and copolymerization promoted by C_1-symmetric zirconocene catalysts. The anion $[CH_3B(C_6F_5)_3]^-$ was included in order to take into account its effect.

Scheme 3. Representation of the Relationship between Energy Barrier and Bond Strength (see Scheme 2 for numbering of atoms)

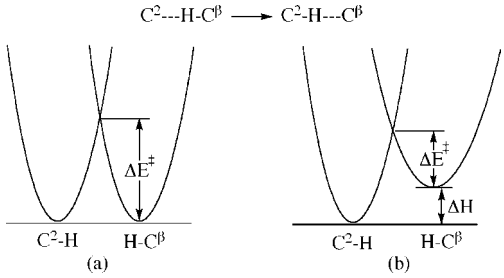

Scheme 4. Active Region of the π-Complex in the 1,2-Insertion Reaction

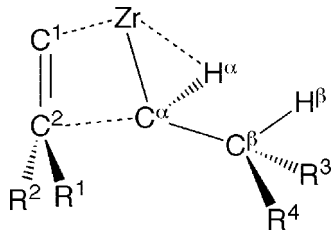

Table 4. Energetics vs Substituents of Olefin and Growing Chain in 1,2-Insertion

	R^1	R^2	R^3	R^4	$\Delta E^{\ddagger}$	ΔH
EE_cis	H	H	H	CH_3	2.69	−8.35
EP_cis	H	H	CH_3	CH_3	4.36	−9.64
PE_cis	H	CH_3	H	CH_3	5.53	−4.33
PP_cis	H	CH_3	CH_3	CH_3	6.70	−2.74

The energy barrier for the chain transfer reaction is found to correlate with the substituents on the C atoms between which the H^{β} atom is migrating (C^2 of the olefin and C^{β} of the growing chain). The reason for this correlation is that the substituents on the C atoms can influence the strength of the C−H bond that is cleaved ($C^{\beta}-H^{\beta}$) and the C−H bond that is formed (C^2-H^{β}). Since increasing substitution on the carbon of a C−H link will decrease the C−H bond strengths, increasing substitution on C^{β} and decreasing substitution on C^2 will lead to a more favorable heat of reaction for β-H transfer. The more favorable heat of reaction will in turn result in a lower barrier of activation, as demonstrated in Scheme 3. Thus the barrier for β-hydrogen transfer follows the order PE > PP > EE > EP.

The chain propagation shows a different dependence on the substituents on C^2 of the olefin and C^{β} of the growing chain. Our calculations indicate that the EE model system, which has a primary olefin C^2 atom and a secondary C^{β} of the growing chain, has the lowest energy barrier for the chain propagation, while the PP system, in which there is one secondary C^2 atom and one tertiary C^{β}, is found with the highest energy barrier of 6.70 kcal/mol. Thus the insertion barrier increases with the number of substituents on C^2 and C^{β} in the order PP > PE > EP > EE.

The different dependence of the energy barriers for the chain propagation and chain transfer reactions on the C^2 and C^{β} substituents leads to different propensities of the four model systems toward the two pathways. Thus, in the EE, PP, and PE systems, chain propagation dominates over chain transfer, while in the EP system, the two pathways become kinetically competitive. Therefore, one can expect that in ethylene−propylene copolymerization (EP system), the strongly favorable chain transfer pathway results in polymers with low molecular weight. On the other hand, ethylene homopolymerization (EE) and propylene homopolymerization (PP) are characterized by relatively higher barriers for β-H transfer than for propagation. Both processes will as a result afford high molecular weight polymers. We shall in a later study explore ways in which we can increase the molecular weight in ethylene−propylene copolymerization. It will also be explored whether C_s- and C_2-symmetric zirconocenes exhibit the same trends with respect to the barriers of insertion and termination.

Acknowledgment. We would like to thank Total for support. T.Z. thanks the Canadian government for a Canada Research Chair.

Supporting Information Available: QM/MM total energies and coordinates for all of the stationary points. This material is available free of charge via the Internet at http://pubs.acs.org.

OM800290N